

Cite this: *Chem. Sci.*, 2021, **12**, 3977

All publication charges for this article have been paid for by the Royal Society of Chemistry

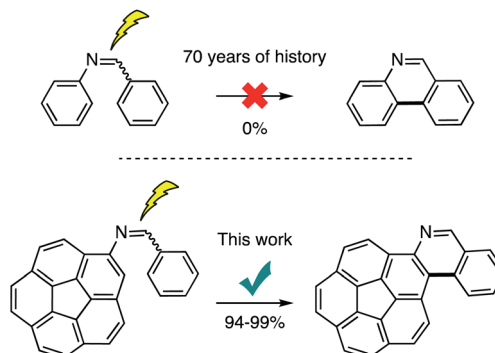
Received 9th December 2020
Accepted 22nd January 2021DOI: 10.1039/d0sc06730j
rsc.li/chemical-science

Introduction

Diarylethenes/stilbenes are known to undergo a *trans*-to-*cis* isomerization upon irradiation with light. The photochemically produced *cis* isomer can undergo a further 6 π -electron cyclization process followed by oxidation to form phenanthrene.¹⁻⁴ This reaction was discovered in 1950.⁵ However, it was poorly understood and remained obscure until Mallory postulated the reversible formation of the dihydrophenanthrene intermediate that could be oxidized to the fully aromatic structure.⁶⁻⁸ This work demonstrated the need for an oxidant. Mallory established that a catalytic amount of iodine was key to the synthesis. The generated hydrogen iodide (HI) is oxidized back to iodine by oxygen for the catalytic cycle to continue. Since that discovery, the reaction has been known as Mallory reaction. The strong acid (HI) formed under Mallory conditions, however, posed threats of side reactions and lowered the isolated yields. In 1991, Katz's group alleviated this situation by incorporating methyloxirane as an acid quencher to the synthetic protocol.⁹ Under this condition, however, a stoichiometric amount of iodine is required as HI is irreversibly consumed. A beneficial attribute of this variation is that oxygen is no longer required and the reaction can be performed under inert conditions. This

eliminates possible side-reactions of typically electron rich aromatics with oxygen. Therefore, high yields can be obtained. It is this practicality that allows for daunting synthetic targets to be prepared through Mallory reaction. This can be seen in Bunz's N-heteroarene,¹⁰ Morin's graphene nano-ribbons,¹¹ Matsuda's [7]helicene,¹² Durola's double [7]helicene,¹³ Fujita's [16]helicene,¹⁴ Nuckolls hexabenzocoronenes,¹⁵ Mallory's phenacenes,¹⁶ Autschbach, Crassous, and Réau's metal-lahelicenes,¹⁷ and corannurylene pentapetalae¹⁸ syntheses employing the photochemical reaction as a key component in the construction of complex aromatic scaffolds.

Despite this success, application of stilbene imines as precursors to prepare aza-based aromatic scaffolds is not

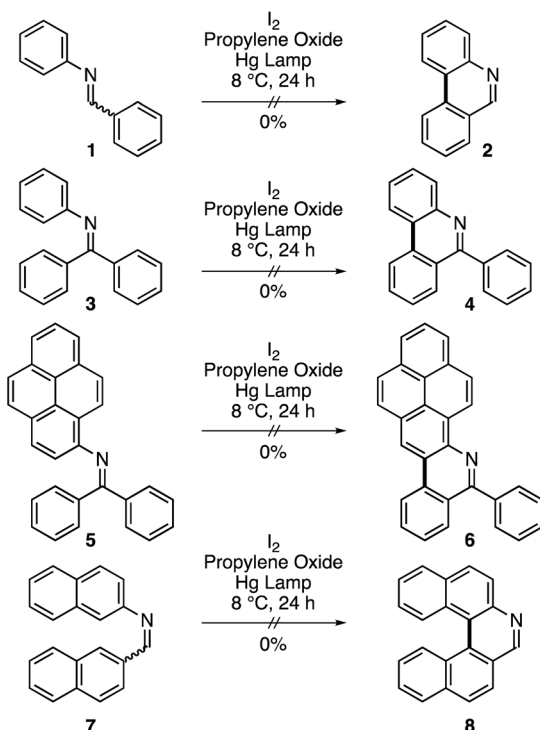


Scheme 1 Stilbene imines are known not to undergo the Mallory reaction (top). Corannulene substrates offer an exception and allow development of the first general and practical photochemical synthesis of azahelicenes through Mallory reaction of the imine precursors (bottom).

^aDivision of Chemistry and Biological Chemistry, School of Physical and Mathematical Sciences, Nanyang Technological University, 21 Nanyang Link, Singapore, 637371 Singapore. E-mail: mstuparu@ntu.edu.sg

^bInstitute of Organic Chemistry, Research Centre for Natural Sciences, Magyar Tudósok Körútja 2, H-1117 Budapest, Hungary

† Electronic supplementary information (ESI) available. CCDC 2038554. For ESI and crystallographic data in CIF or other electronic format see DOI: [10.1039/d0sc06730j](https://doi.org/10.1039/d0sc06730j)



Scheme 2 Mallory reaction of imine precursors.

feasible (Scheme 1). For instance, it is known that imine **1** fails to produce phenanthridine **2** (Scheme 2).^{8,19} We have repeated this reaction with exposure time of 24 hours and found it unsuccessful. It has been suggested that a rapid photo-isomerization in stilbene imines (half-life = 1 s)²⁰ may not give the *cis* isomer a chance to cyclize.¹ This hypothesis can be tested with the help of imine **3** in which the *cis* configuration is built in by molecular design.²¹ However, no product (**4**) could be detected after 24 hours of exposure time.

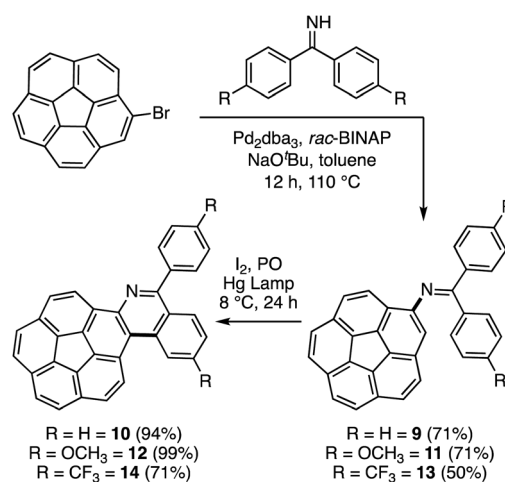
We have added one more compound to this series with the help of a planar extended aromatic structure, pyrene. The fate of the photochemical reaction in **5** is the same as **1** and **3** and **6** could not be obtained. Caronna and coworkers have shown that a naphthalene-based imine (**7**) could not be cyclized to **8** under neutral conditions.²² In addition, azobenzene, having both olefin carbon atoms replaced with nitrogen atoms (N=N), is also not known to cyclize under Mallory conditions.²³ In light of these results, it is reasonable to agree with the consensus that stilbene cyclizations takes place through a $^1\pi-\pi^*$ excited state.¹ However, introduction of the lone pair of the electrons of the nitrogen atom(s) results in $^1n-\pi^*$ becoming the lowest excited state. In this situation, the lowest $^1\pi-\pi^*$ excited state, which is the product-yielding state becomes insignificant as the internal conversion to $^1n-\pi^*$ is a fast process resulting in a rapid decay of the photoexcitation energy. The support for this notion comes from the fact that once the nitrogen atom(s) are engaged by protonation²⁴⁻²⁶ or co-ordination^{27,28} then the photocyclization proceeds albeit with low yields. The protonation in imines is particularly not helpful as it favors the decomposition *via* hydrolysis over photocyclization. It is due to this reason that

although the photochemical cyclizations are a dominant force in the synthesis of helicenes²⁹⁻³⁴ (in which the phenanthrene motif repeats in the molecular structure) azahelicenes have never been prepared in the past 70 years by the classic Mallory reaction of imine precursors.³⁵⁻³⁸ Here, we show for the very first time that single and double azahelicenes can be prepared photochemically in high yields through use of corannulene-based stilbene-like imine precursors. A plausible explanation for this anomaly would be that the curved aromatic substituent, corannulene, helps to override the $n-\pi^*$ internal conversion process by lowering the product yielding $\pi-\pi^*$ excited state. At this moment, however, this notion remains a hypothesis due to difficulties in obtaining an unequivocal proof through theory or experimental work.

Results and discussion

Initially, commercially available benzophenone imine and bromocorannulene³⁹ were subjected to a palladium-catalyzed amination reaction as described by Buchwald and coworkers (Scheme 3).⁴⁰ This reaction provided the simplest corannulene imine scaffold (**9**) in 71% isolated yield. An oxidative photocyclization of **9** with the help of a medium-pressure Hg lamp (125 W) provided the azaphenanthrene **10** in 94% isolated yield. In X-ray crystallography, the two azahelicene enantiomers are observed to pack in two columns (Fig. 1). In these columns, the molecules interact with a $\pi-\pi$ stacking interaction (3.17 Å), a bifurcated CH- π interaction (2.80 and 2.78 Å), and a single CH- π interaction (2.76 Å). The central bowl-depth (0.85 Å) is not affected significantly as a result of helicene formation (Fig. S1†).⁴¹

Encouraged by the aforementioned results, a variation in the substitution pattern is sought with the help of imines **11** and **13** carrying electron donating and withdrawing methoxy and trifluoromethyl substituents, respectively (Scheme 3). For this, a simple synthesis of the required diphenyl ketamines is carried out through reacting methoxybenzonitrile and



Scheme 3 Synthesis of corannulene-based imine precursors and their application in oxidative photocyclizations to yield single azahelicenes (PO = propylene oxide).



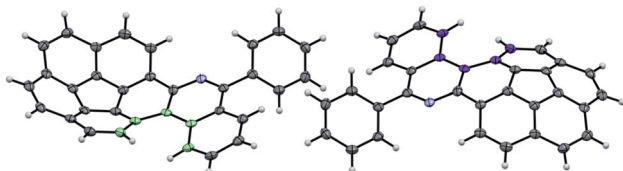


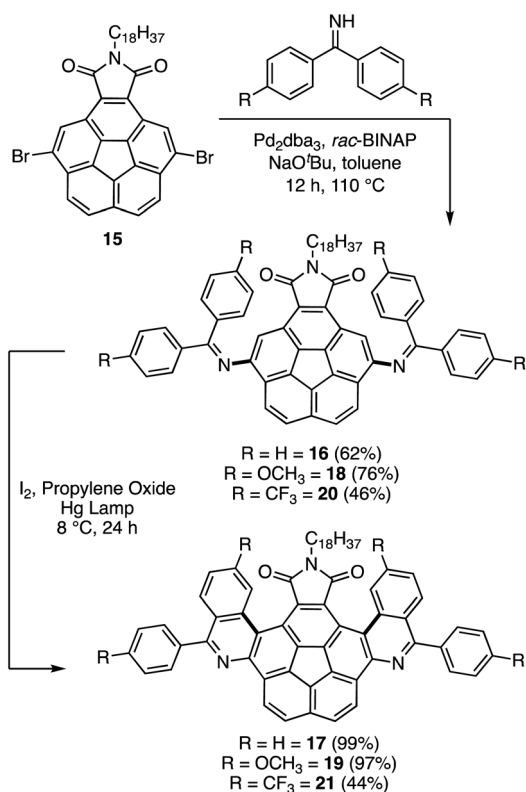
Fig. 1 ORTEP representation of a pair of enantiomers of **10** with 50% probability of ellipsoids. The M and P [4]helicenes are shown with purple and green colors, respectively.

trifluoromethylbenzonitrile with the appropriate arylmagnesium bromide reagent. While the other imines were stable, the electron deficient imine **13** was found to be unstable. Therefore, it was freshly prepared before the amination reaction. The oxidative photocyclizations proceeded smoothly in the case of **12** with an isolated yield of 99%. However, the decomposition of the imine **13** lowers the yield for the formation of **14** to 71%. Nonetheless, the photochemical cyclization itself is not deterred by the presence of active electronic functionalities.

To further probe the generality of the concept, a more demanding system carrying two imines was explored. In this system, Sygula's dicarboxylate-derived imide **15** was used as the substrate for the amination reaction to yield **16** in 62% isolated yield (Scheme 4).^{42,43} A subsequent photocyclization gave double helicene **17** in 99% isolated yield. Similar results were obtained in the case of methoxy derivative **18** (97%). However, once again, the

electron poor CF_3 derivative afforded low yields (46 and 44% for **20** and **21**, respectively) because of the decomposition of the imine. The long alkyl chain ($\text{C}_{18}\text{H}_{37}$) on the imide group aids the solubility for the synthesis and characterization of the compounds.

The curved corannulene fragment in the prepared molecules resembles the cap region of fullerene C_{60} .^{44–54} The structural resemblance also manifests in its electronic properties. For instance, corannulene is an acceptor of electrons. With a doubly degenerate LUMO, corannulene can accept up to 4 electrons (0.2 e^- per carbon atom)^{55,56} while C_{60} with a triply degenerate LUMO accepts up to 6 electrons (0.1 e^- per carbon atom). However, the electron affinity of corannulene is not as high as fullerene C_{60} . Therefore, there is a large effort in molecular engineering of the corannulene scaffold to enhance its reduction potential.⁵⁷ Having practical access to the π -extended compounds, their electron affinity was studied with the help of square-wave voltammetry (SWV) and cyclic voltammetry (CV) in dimethylformamide (Fig. 2, Table 1 and Fig. S2–S7†). Cyclic voltammetry measurements indicated that compounds **10**, **12**, **14**, **17**, **19**, and **21** all undergo chemically reversible one-electron reduction processes with the reductive (E_p^{red}) and oxidative (E_p^{ox}) peaks having approximately equal reductive (i_p^{red}) and oxidative (i_p^{ox}) peak currents ($i_p^{\text{red}}/i_p^{\text{ox}} \approx 1$) at a scan rate (v) of 0.1 V s^{-1} . Five compounds, namely **10**, **12**, **17**, **19**, and **21** underwent a second chemically reversible or partially chemically reversible one-electron reduction process at approximately 0.5 V more negative than the first electron transfer.



Scheme 4 Synthesis of double azahelicenes through Mallory reaction of corannulene-based imine precursors.

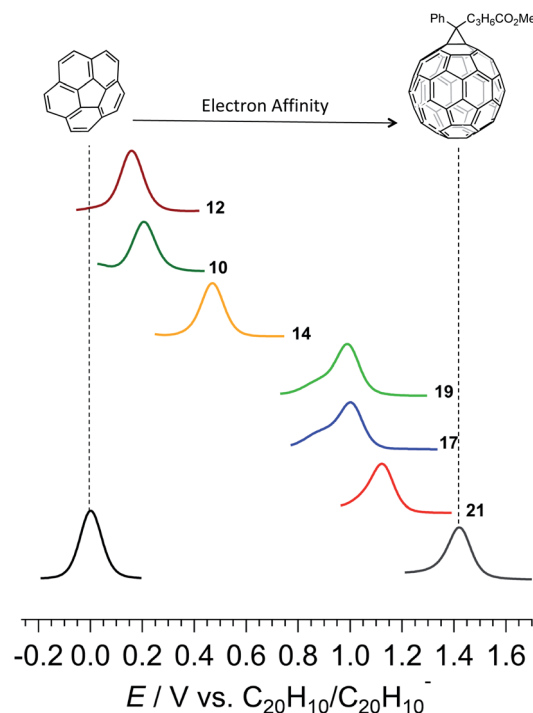


Fig. 2 Square-wave voltammetry at a 1 mm diameter glassy carbon electrode showing reduction processes of 1 mM corannulene, PC_{61}BM , and the synthesized azahelicenes in DMF containing $0.1 \text{ M} n\text{-Bu}_4\text{NPF}_6$. The compound numbers are shown at the end of the data trace.

Table 1 Measured reduction processes by SWV of studied compounds. Voltammetric measurements were conducted in a Faraday cage with a 1 mm diameter planar GC working electrode in DMF containing 1 mM of compound and 0.1 M n Bu₄NPF₆ at 298 \pm 2 K. All values are referenced to the Fc/Fc⁺ redox couple. The orbital energies were calculated using Def2TZVPP basis set

Compound	$E_{\text{red}}^1/\text{V}$	$E_{\text{red}}^2/\text{V}$	HOMO (eV)	LUMO (eV)
21	-1.19	-1.72	-8.28	-1.74
17	-1.32	-1.87	-7.71	-1.32
19	-1.33	-1.87	-7.30	-1.11
14	-1.85	—	-8.14	-0.92
10	-2.11	-2.51	-7.74	-0.51
12	-2.16	-2.64	-7.44	-0.37

Furthermore, the compounds also underwent further reduction processes at more negative potentials, but these were all chemically irreversible and were thus likely associated with the reduction of reaction products formed by decomposition of the heavily reduced species (Fig. S2–S7†).

A trend can be seen in which the electron rich methoxy group lowers while the electron withdrawing trifluoromethyl enhances the electron affinity of the material, as evidenced by the shift in reduction potentials of the compounds (Fig. 2 and Table 1). A comparatively higher electron affinity of the double helicenes stems from a combination of a larger aromatic area, a higher number of trifluoromethyl substituents, and the presence of the electron withdrawing imide group. In comparison to pristine corannulene, **21** exhibits an anodic shift of 1.1 V in its first reduction potential. Such high electron affinities are hallmarks of fullerene and its derivatives, which find extensive applications in organic electronics. Even so, the highest electron affinity double azahelicene **21** falls short by 0.3 V to reach the prevalent fullerene-based electron acceptor, phenyl-C₆₁-butyric acid methyl ester, commonly known as PC₆₁BM in the arena of organic electronics. The advantage of the present system is a high solubility in a range of common laboratory solvents, and modularity of the synthesis which allows control over placement, number, and nature of a substituent and hence the material properties.

DFT calculations were carried out to explore the conformational behaviour and evaluate the electronic structure of the obtained products (Fig. S8–S10†). The structures were optimized at the ω B97X-D/Def2SVP level of theory. The frontier molecular orbital (HOMO and LUMO) energies were calculated at the ω B97X-D/Def2TZVPP level. For single azahelicenes, both the HOMO and LUMO are delocalized over the entire molecule as illustrated in Fig. 3 (top) (Fig. S8† for **12** and **14**). In this class, the LUMO of MeO-substituted **12** is found to be the highest in energy while **14** bearing electron-withdrawing CF₃ groups exhibits the lowest LUMO energy. This is in line with the voltammetric measurements as the experimental redox potential of **12** points to a decreased propensity for reduction in reference to **10**. For **14**, the experimental redox potential indicates that the reduction process is favoured as compared to **10** and **12** derivatives. The HOMO–LUMO energy gaps of the parent molecule **10** and CF₃-substituted **14** are predicted to be nearly identical (7.23 eV and 7.22 eV, respectively), whereas this energy gap

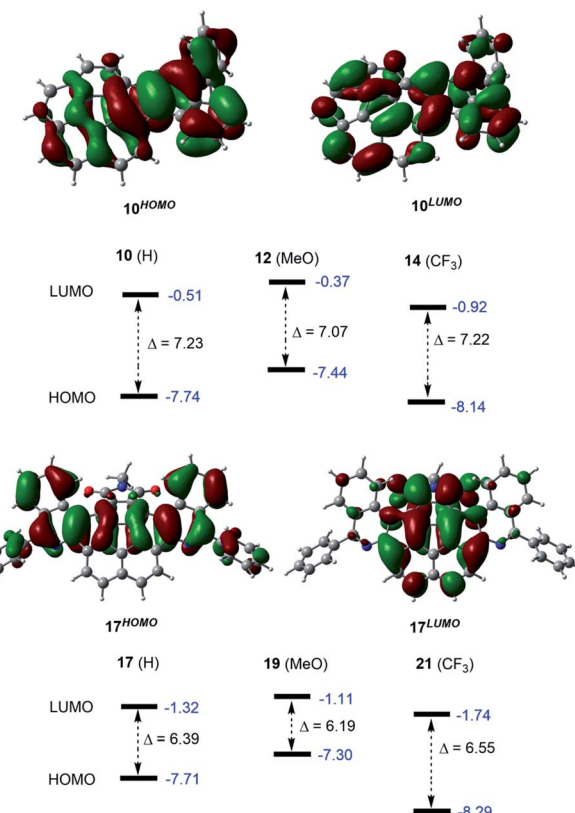


Fig. 3 Frontier molecular orbitals for **10** (top) and **17** (bottom) (isovalue = 0.03). Orbital energies (highlighted in blue) and the HOMO–LUMO energy gaps (Δ) are given in eV.

decreases to 7.07 eV for **12**. In the case of the double azahelicenes, the C₁₈H₃₇ alkyl chain was replaced with a Me-group in the calculations to avoid conformational complexity. In the most stable conformer of **17**, the two isoquinoline moieties reside at the convex face of the corannulene core. Additional conformers of **17** (Fig. S9†) and the structures of **19** and **21** derivatives are presented in the SI along with their calculated HOMO and LUMO energies (Fig. S10†). The HOMO of **17** is longitudinally delocalized through the center of the molecule, as shown in Fig. 3 (bottom). By contrast, the LUMO is vertically distributed over the corannulene core and the succinimide fragment. The pattern of the HOMO–LUMO lobes remains unchanged when either MeO- or CF₃-substituents are incorporated into the parent molecule **17** (Fig. S10† for **19** and **21**). Again, the measured redox potentials are in accordance with the calculated LUMO energy trends. The LUMO of **21**, possessing four electron-withdrawing CF₃-substituents, was predicted to be the lowest, suggesting an increased electron affinity, as opposed to **19** with four MeO-groups, the LUMO of which lies higher than that of **17** and **21**. The energy gap between the HOMO and LUMO is predicted to be 6.39 eV for **17**, and it decreases to 6.19 eV in the case of **19**. This energy gap increases to 6.55 eV in derivative **21**. In addition, the HOMO–LUMO energy gaps of double azahelicenes were found to be smaller than those of single azahelicenes.

Lastly, DFT computations also enabled us to examine the dynamic nature of the corannulene derivatives **17** and **10**. The



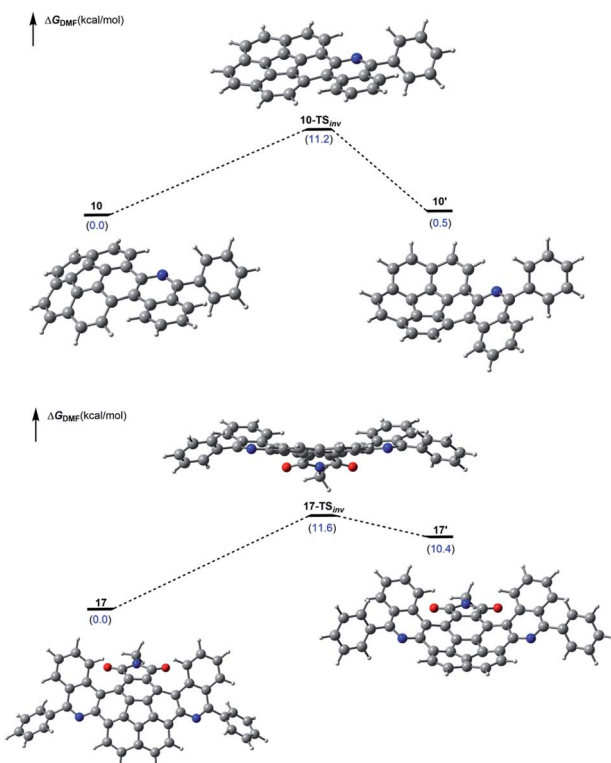


Fig. 4 Free energy profile of a computationally identified bowl inversion processes in **10** (top) and **17** (bottom). Relative stabilities are given in parenthesis (in kcal mol^{-1}) with respect to the most stable conformer.

transition state corresponding to the bowl-inversion appears energetically accessible in both cases, and the calculated inversion barriers are predicted to be nearly identical (Fig. 4).

Conclusions

In summary, corannulene substrates offer the very first imine precursors to successfully undergo the oxidative cyclization process to furnish single and double azahelicenes in isolated yields of >90%. The chemistry is modular and allows for control over the substitution pattern and therefore properties of the curved π -scaffolds. We envisage that the efficient synthesis of azahelicene reported here coupled with electron affinity of the central aromatic bowl may provide an interesting ligand for the preparation of metallahelicenes^{17,58–62} or metal organic frameworks with anticipation of new properties and functions.^{63,64} These results also provide an impetus for a comprehensive theoretical treatment of the subject in order to understand the reason behind the anomalous behavior of the curved corannulene nucleus in imine-based Mallory cyclizations.⁶⁵

Experimental details

General procedure for the synthesis of imine precursors

A solution (5 mL) of tris(dibenzylideneacetone)dipalladium(0) (0.015 mmol) and *rac*-BINAP (0.03 mmol) in toluene was purged with nitrogen, and stirred at 110 °C for 30 min. After cooling to

room temperature, a mixture of benzophenone imine (0.378 mmol), sodium *tert*-butoxide (0.378 mmol) and bromocorannulene (or aryl bromide) (0.303 mmol) was added and the mixture was stirred at 110 °C overnight. The mixture was cooled to room temperature, diluted with CH_2Cl_2 , filtered through a pad of Celite, and evaporated to dryness. The residue was subjected to column chromatography on silica gel using a mixture of CH_2Cl_2 /hexane as eluent, to give the imine with isolated chemical yields ranging from 61 to 81%.

General procedure for the synthesis of single aza[4]helicenes

A solution of imine precursor (0.105 mmol), iodine (0.115 mmol), and propylene oxide (3.15 mmol) in 120 mL of toluene was irradiated in a photoreactor fitted with a water-cooled (8 °C) immersion flask and a medium-pressure Hg lamp (125 W) under N_2 atmosphere. After completion (28 h, monitored by TLC) toluene was evaporated under reduced pressure. The residue was quenched with saturated aqueous $\text{Na}_2\text{S}_2\text{O}_3$ solution and extracted with dichloromethane (2×20 mL). The CH_2Cl_2 extracts were combined, dried over Na_2SO_4 , filtered and evaporated. The residue was subjected to column chromatography on silica gel using a mixture of CH_2Cl_2 /hexane as eluent, to give the single aza[4]helicene with isolated chemical yields ranging from 71 to 99%.

General procedure for the synthesis of diimine precursors

A solution (5 mL) of tris(dibenzylideneacetone)dipalladium(0) (0.013 mmol) and *rac*-BINAP (0.027 mmol) in toluene was purged with nitrogen, and stirred at 110 °C for 30 min. After cooling to room temperature, a mixture of benzophenone imine (0.30 mmol), sodium *tert*-butoxide (0.30 mmol) and dibromocorannulene derivative **15** (0.137 mmol) was added and the mixture was stirred at 110 °C for 8 h. The mixture was cooled to room temperature, diluted with CH_2Cl_2 , filtered through a pad of Celite, and evaporated to dryness. The residue was subjected to column chromatography on silica gel using a mixture of CH_2Cl_2 /hexane as eluent, to give the diimine precursor with isolated chemical yields ranging from 46 to 76%.

General procedure for the synthesis of double aza[4]helicenes

A solution of precursor diimine (0.075 mmol), iodine (0.165 mmol), and propylene oxide (4.5 mmol) in 120 mL of toluene was irradiated in a photoreactor fitted with a water-cooled (8 °C) immersion flask and a medium-pressure Hg lamp (125 W) under N_2 atmosphere. After completion (24 h, monitored by TLC) toluene was evaporated under reduced pressure. The residue was quenched with saturated aqueous $\text{Na}_2\text{S}_2\text{O}_3$ solution and extracted with dichloromethane (2×20 mL). The CH_2Cl_2 extracts were combined, dried over Na_2SO_4 , filtered and evaporated. The residue was subjected to column chromatography on silica gel using a mixture of CH_2Cl_2 /hexane as eluent, to give the double aza[4]helicene with isolated chemical yields ranging from 44 to 99%.

Conflicts of interest

There are no conflicts to declare.

Acknowledgements

Financial support from the Ministry of Education Singapore under the AcRF Tier 1 (2019-T1-002-066) (RG106/19) (2018-T1-001-176) (RG18/18); Agency for Science, Technology and Research (A*STAR)-AME IRG A1883e0006; and NTU (04INS000171C230) is gratefully acknowledged. Computer facilities provided by NIIF HPC Hungary (project 85708 katapro) are also acknowledged. Dr Yongxin Li's efforts in conducting X-ray crystallographic measurement are highly appreciated. The authors thank Dr A. A. Dar for help with the synthesis of fluorinated compounds.

Notes and references

- 1 F. B. Mallory and C. W. Mallory, Photocyclization of Stilbenes and Related Molecules, in *Organic Reactions*, Wiley, New York, 1984, vol. 30.
- 2 N. Hoffmann, *Chem. Rev.*, 2008, **108**, 1052–1103.
- 3 K. B. Jørgensen, *Molecules*, 2010, **15**, 4334–4358.
- 4 A. G. Lvov, *J. Org. Chem.*, 2020, **85**, 8749–8759.
- 5 C. O. Parker and P. Spoerri, *Nature*, 1950, 603.
- 6 F. B. Mallory, C. S. Wood, J. T. Gordon, L. C. Lindquist and M. L. Savitz, *J. Am. Chem. Soc.*, 1962, **84**, 4361–4362.
- 7 F. B. Mallory, J. T. Gordon and C. S. Wood, *J. Am. Chem. Soc.*, 1963, **85**, 828–829.
- 8 F. B. Mallory, C. S. Wood and J. T. Gordon, *J. Am. Chem. Soc.*, 1964, **86**, 3094–3102.
- 9 L. Liu, B. Yang, T. J. Katz and M. K. Poindexter, *J. Org. Chem.*, 1991, **56**, 3769–3775.
- 10 A. H. Endres, M. Schaffroth, F. Paulus, H. Reiss, H. Wadeppohl, F. Rominger, R. Krämer and U. H. F. Bunz, *J. Am. Chem. Soc.*, 2016, **138**, 1792–1795.
- 11 A. Jolly, D. Miao, M. Daigle and J. F. Morin, *Angew. Chem., Int. Ed.*, 2019, **59**, 4624–4633.
- 12 Y. Nakakuki, T. Hirose, H. Sotome, H. Miyasaka and K. Matsuda, *J. Am. Chem. Soc.*, 2018, **140**, 4317–4326.
- 13 M. Ferreira, G. Naulet, H. Gallardo, P. Dechambenoit, H. Bock and F. Durola, *Angew. Chem., Int. Ed.*, 2017, **56**, 3379–3382.
- 14 K. Mori, T. Murase and M. Fujita, *Angew. Chem., Int. Ed.*, 2015, **54**, 6847–6851.
- 15 S. Xiao, J. Tang, T. Beetz, X. Guo, N. Tremblay, T. Siegrist, Y. Zhu, M. Steigerwald and C. Nuckolls, *J. Am. Chem. Soc.*, 2006, **128**, 10700–10701.
- 16 F. B. Mallory, K. E. Butler, A. C. Evans, E. J. Brondyke, C. W. Mallory, C. Yang and A. Ellenstein, *J. Am. Chem. Soc.*, 1997, **119**, 2119–2124.
- 17 L. Norel, M. Rudolph, N. Vanthuyne, J. A. G. Williams, C. Lescop, C. Roussel, J. Autschbach, J. Crassous and R. Réau, *Angew. Chem., Int. Ed.*, 2009, **49**, 99–102.
- 18 D. Meng, G. Liu, C. Xiao, Y. Shi, L. Zhang, L. Jiang, K. K. Baldridge, Y. Li, J. S. Siegel and Z. Wang, *J. Am. Chem. Soc.*, 2019, **141**, 5402–5408.
- 19 P. Hugelshofer, J. Kalvoda and K. Schaffner, *Helv. Chim. Acta*, 1960, **43**, 1322–1332.
- 20 D. G. Anderson and G. Wettermark, *J. Am. Chem. Soc.*, 1965, **87**, 1433–1438.
- 21 F. B. Mallory and C. Wood, *Tetrahedron Lett.*, 1965, **30**, 2643–2648.
- 22 S. Abbate, C. Bazzini, T. Caronna, F. Fontana, C. Gambarotti, F. Gangemi, G. Longhi, A. Mele, I. N. Sora and W. Panzeri, *Tetrahedron*, 2006, **62**, 139–148.
- 23 G. E. Lewis, *J. Org. Chem.*, 1960, **25**, 2193–2195.
- 24 G. E. Lewis, *Tetrahedron Lett.*, 1960, 12–13.
- 25 G. M. Badger, C. P. Joshua and G. Lewis, *Tetrahedron Lett.*, 1964, **5**, 3711–3713.
- 26 T. Caronna, S. Gabbiadini, A. Mele and F. Recupero, *Helv. Chim. Acta*, 2002, **85**, 1–8.
- 27 S. Prabhakar, A. M. Lobo and M. R. Tavares, *J. Chem. Soc., Chem. Commun.*, 1978, 884–885.
- 28 T. Murase, T. Suto and H. Suzuki, *Chem.-Asian J.*, 2017, **12**, 726–729.
- 29 A. Urbano, *Angew. Chem., Int. Ed.*, 2003, **42**, 3986–3989.
- 30 T. Katz, *Angew. Chem., Int. Ed.*, 2000, **39**, 1921–1923.
- 31 W.-B. Lin, M. Li, L. Fang and C.-F. Chen, *Chin. Chem. Lett.*, 2018, **29**, 40–46.
- 32 M. Gingras, *Chem. Soc. Rev.*, 2013, **42**, 1051–1095.
- 33 Y. Shen and C.-F. Chen, *Chem. Rev.*, 2012, **112**, 1463–1535.
- 34 C.-F. Chen and Y. Shen, *Helicene Chemistry*, Springer, Berlin, Heidelberg, 2016.
- 35 K. Dhibaibi, L. Favereau and J. Crassous, *Chem. Rev.*, 2019, **119**, 8846–8953.
- 36 F. Dumitrescu, D. G. Dumitrescu and I. Aron, *ARKIVOC*, 2010, 1–32.
- 37 C. Bazzini, S. Brovelli, T. Caronna, C. Gambarotti, M. Giannone, P. Macchi, F. Meinardi, A. Mele, W. Panzeri, F. Recupero, A. Sironi and R. Tubino, *Eur. J. Org. Chem.*, 2005, **2005**, 1247–1257.
- 38 T. Caronna, F. Fontana, A. Mele, I. Sora, W. Panzeri and L. Viganò, *Synthesis*, 2008, **2008**, 413–416.
- 39 T. J. Seiders, E. L. Elliott, G. H. Grube and J. S. Siegel, *J. Am. Chem. Soc.*, 1999, **121**, 7804–7813.
- 40 J. P. Wolfe, J. Åhman, J. P. Sadighi, R. A. Singer and S. L. Buchwald, *Tetrahedron Lett.*, 1997, **38**, 6367–6370.
- 41 CCDC 2038554† contains the crystallographic data.
- 42 A. Sygula, S. D. Karlen, R. Sygula and P. W. Rabideau, *Org. Lett.*, 2002, **4**, 3135–3137.
- 43 R.-Q. Lu, W. Xuan, Y.-Q. Zheng, Y.-N. Zhou, X.-Y. Yan, J.-H. Dou, R. Chen, J. Pei, W. Weng and X.-Y. Cao, *RSC Adv.*, 2014, **4**, 56749–56755.
- 44 L. T. Scott, *Pure Appl. Chem.*, 1996, **68**, 291–300.
- 45 V. M. Tsefrikas and L. T. Scott, *Chem. Rev.*, 2006, **106**, 4868–4884.
- 46 A. Sygula, *Eur. J. Org. Chem.*, 2011, 1611–1625.
- 47 Y.-T. Wu and J. S. Siegel, *Top. Curr. Chem.*, 2014, **349**, 63–120.
- 48 B. M. Schmidt and D. Lentz, *Chem. Lett.*, 2014, **43**, 171–177.
- 49 A. Sygula, *Synlett*, 2016, **27**, 2070–2080.



50 A. M. Rice, E. A. Dolgopolova and N. B. Shustova, *Chem. Mater.*, 2017, **29**, 7054–7061.

51 M. Saito, H. Shinokubo and H. Sakurai, *Mater. Chem. Front.*, 2018, **2**, 635–661.

52 A. V. Zabula, S. N. Spisak, A. S. Filatov, A. Y. Rogachev and M. A. Petrukhina, *Acc. Chem. Res.*, 2018, **51**, 1541–1549.

53 E. Nestoros and M. C. Stuparu, *Chem. Commun.*, 2018, **54**, 6503–6519.

54 E. M. Muzammil, D. Halilovic and M. C. Stuparu, *Commun. Chem.*, 2019, 1–13.

55 A. Ayalon, M. Rabinovitz, P. C. Cheng and L. T. Scott, *Angew. Chem., Int. Ed.*, 1992, **31**, 1636–1637.

56 A. Aylon, A. Sygula, P.-C. Cheng, M. Rabinovitz, P. W. Rabideau and L. T. Scott, *Science*, 1994, **265**, 1065–1067.

57 A. Haupt and D. Lentz, *Chem.-Eur. J.*, 2019, **25**, 3440–3454.

58 N. Saleh, C. Shen and J. Crassous, *Chem. Sci.*, 2014, **5**, 3680–3694.

59 E. Anger, M. Rudolph, L. Norel, S. Zrig, C. Shen, N. Vanthuyne, L. Toupet, J. A. G. Williams, C. Roussel, J. Autschbach, J. Crassous and R. Réau, *Chem.-Eur. J.*, 2011, **17**, 14178–14198.

60 E. Anger, M. Rudolph, C. Shen, N. Vanthuyne, L. Toupet, C. Roussel, J. Autschbach, J. Crassous and R. Réau, *J. Am. Chem. Soc.*, 2011, **133**, 3800–3803.

61 C. Shen, E. Anger, M. Srebro, N. Vanthuyne, L. Toupet, C. Roussel, J. Autschbach, R. Réau and J. Crassous, *Chem.-Eur. J.*, 2013, **19**, 16722–16728.

62 C. Shen, E. Anger, M. Srebro, N. Vanthuyne, K. K. Deol, T. D. Jefferson, G. Muller, J. A. G. Williams, L. Toupet, C. Roussel, J. Autschbach, R. Réau and J. Crassous, *Chem. Sci.*, 2014, **5**, 1915–1927.

63 W. B. Fellows, A. M. Rice, D. E. Williams, E. A. Dolgopolova, A. K. Vannucci, P. J. Pellechia, M. D. Smith, J. A. Krause and N. B. Shustova, *Angew. Chem., Int. Ed. Engl.*, 2016, **55**, 2195–2199.

64 A. M. Rice, W. B. Fellows, E. A. Dolgopolova, A. B. Greytak, A. K. Vannucci, M. D. Smith, S. G. Karakalos, J. A. Krause, S. M. Avdoshenko, A. A. Popov and N. B. Shustova, *Angew. Chem., Int. Ed.*, 2017, **56**, 4525–4529.

65 I. Fernández, *Chem. Sci.*, 2020, **11**, 3769–3779.

